Hindawi Publishing Corporation
Advances in Materials Science and Engineering
Volume 2014, Article ID 489701, 6 pages
http://dx.doi.org/10.1155/2014/489701

Research Article

Effect of Nd Addition on the Microstructure and Martensitic Transformation of Ni-Ti Shape Memory Alloys

M. Dovchinvanchig,[1,2] C. W. Zhao,[1] S. L. Zhao,[1] X. K. Meng,[1] Y. J. Jin,[1] and Y. M. Xing[1]

[1] *College of Science, Inner Mongolia University of Technology, Hohhot 010051, China*
[2] *Institute of Physics and Technology, Mongolian Academy of Sciences, 210351 Ulaanbaatar, Mongolia*

Correspondence should be addressed to C. W. Zhao; cwzhao@aliyun.com

Received 19 February 2014; Revised 18 April 2014; Accepted 2 May 2014; Published 20 May 2014

Academic Editor: Shuichi Miyazaki

The effect of rare earth element Nd addition on the microstructure and martensitic transformation behavior of $Ni_{50}Ti_{50-x}Nd_x$ ($x = 0, 1, 3, 7, 20$) shape memory alloy was investigated experimentally. The results showed that the microstructure of Ni-Ti-Nd ternary alloy consists of the NiNd phase and the NiTi matrix. One-step martensitic transformation was observed in all alloys. The martensitic transformation start temperature M_s increased gradually with increasing Nd content for Ni-Ti-Nd alloys.

1. Introduction

Ni-Ti based shape memory alloys (SMAs) have unique shape memory effects and super-elasticity behavior and have been used in various fields, particularly in engineering and medical applications [1]. Current research interest on SMAs mainly lies in controlling the martensitic transformation temperature and improving the shape memory effect for their applications. The effects of martensitic transformation, super-elasticity, and shape memory have been widely studied by adding transitional elements to Ni-Ti binary alloys. These elements include Fe [2], Hf [3], and Pd [4]. It is found that most alloying elements such as Fe lower martensitic transformation temperature, but there are only a few, such as Hf and Pd, which increase martensitic transformation temperature [5].

Moreover, the microstructure and martensitic transformation temperature of the rare earth (RE) of Ce [6], Gd [7], Dy [8], and La [9] in addition to Ni-Ti binary alloys have also been studied using scanning electron microscopy (SEM), energy dispersive spectrometry (EDS), X-ray diffraction (XRD), and differential scanning calorimetry (DSC). The addition of these REs to Ni-Ti binary alloys was found to increase the martensitic transformation temperature and change the phase transformation sequence.

RE element Nd is also a widely used element, particularly in magnetic materials. However, only few studies have been conducted on Nd addition to shape memory alloy. The only study found in the literature is that on Nd addition to Ni-Ti-Fe alloy, but the Nd fraction is less than 1 at.% [10]. The effect of Nd addition to Ni-Ti binary alloy on microstructure and martensite transformation temperature remains unclear. In this paper, Nd content with atomic fractions of 1%, 3%, 7%, and 20% was added to Ni-Ti binary alloys, and the microstructure and martensitic transformation were studied experimentally.

2. Material and Methods

The $Ni_{50}Ti_{50-x}Nd_x$ alloys were prepared by melting each 10 g of raw materials with different nominal compositions (99.9 mass% sponge Ti, 99.7 mass% electrolytic Ni, and 99.95 mass% Nd) in a nonconsumable arc-melting furnace using a water-cooled copper crucible. The alloys are denoted by Nd0, Nd1, Nd3, Nd7, and Nd20 to refer to $Ni_{50}Ti_{50}$, $Ni_{50}Ti_{49}Nd_1$, $Ni_{50}Ti_{47}Nd_3$, $Ni_{50}Ti_{43}Nd_7$, and $Ni_{50}Ti_{30}Nd_{20}$ alloys, respectively. Arc-melting was repeated four times to ensure the uniformity of composition. The specimens are spark-cut from the ingots and solution-treated at 850°C for an hour in a quartz tube furnace. Subsequently the specimens

Table 1: Lattice parameters of Ni-Ti-Nd alloys.

Alloy	Phase	a (nm^3)	b (nm^3)	c (nm^3)	β (°)	V (nm^3)	Source
Nd0	M	0.2898	0.4121	0.4619	97.86	0.05464	This work
Nd1	M	0.2904	0.4123	0.4920	98.11	0.05475	
	A	0.3009				0.02724	
Nd3	M	0.2939	0.4124	0.4639	98.39	0.05562	
	A	0.3017				0.02747	
Nd7	M	0.2940	0.4136	0.4650	99.25	0.05579	
	A	0.3021				0.02757	
Nd20	M	0.2948	0.4170	0.4657	99.48	0.05645	
	A	0.3026				0.02771	
NiTi	M	0.2898	0.4108	0.4646	97.78	0.05480	JCPDF card number 65-0145
	A	0.3007				0.02719	JCPDF card number 65-4572
$NiTi_2$		1.131				1.4503	JCPDF card number 72-0442
NiNd		0.3803	1.046	0.4339		0.17262	JCPDF card number 19-0818

were quenched using water. Thereafter, the specimens are mechanically and lightly polished to obtain a plain surface.

The phase transformation temperatures of $Ni_{50}Ti_{50-x}Nd_x$ alloys were determined by DSC using a TA Q2000 calorimeter. The temperature range of heating and cooling was from −30°C to 140°C, and the scanning rate of heating and cooling was 10°C/min. SEM observations were conducted using a FEI Quanta 650 FEG equipped with EDS analysis systems made by Oxford. An XRD experiment was conducted using a D/MAX-2500PC X-ray diffractometer. The transmission electron microscope (TEM) sample was prepared using the standard technique involving mechanical grinding followed by Ar+ ion milling. TEM experiment was conducted on a JEM-2010 TEM at 200 kV. Images were recorded on a Gatan 1k×1k slow scan CCD camera and processed using the Gatan DigitalMicrograph software.

3. Results and Discussion

3.1. Microstructure of $Ni_{50}Ti_{50-x}Nd_x$ Alloy. Figure 1(a) depicts the XRD curves of $Ni_{50}Ti_{50-x}Nd_x (x = 0, 1, 3, 7, 20)$ alloys at room temperature. The diffraction peaks are identified to be from NiTi B19′ martensite phase, NiTi B2 austenite phase, $NiTi_2$ phase, and NiNd alloy after comparing with JCPDF cards (numbers 65-0145, 65-4572, 72-0442, and 19-0818). The detailed crystal plane indices are marked in Figure 1(b) for Nd0 and Figure 1(c) for Nd3, but the relative intensities of each XRD curve are quite different because of the differences in martensite phase fraction and austenite phase fraction. In this paper, the letter M denotes the NiTi B19′ martensite phase and the letter A denotes the NiTi B2 austenite phase. This perspective will be confirmed in the following DSC analysis. Figure 1(d) depicts a comparison of $(111)_M$ diffraction peaks of $Ni_{50}Ti_{50-x}Nd_x (x = 0, 1, 3, 7, 20)$ alloys. The $(111)_M$ peak is observed to move toward the left for $Ni_{50}Ti_{50-x}Nd_x (x = 1, 3, 7, 20)$ alloys; that is, the diffraction angle decreases with increasing Nd fraction, which indicates that the interplanar spacing of (111) of the martensite expands with Nd addition from 1 at.% to 20 at.%. The lattice parameters of alloys can be also calculated by peaks' position in XRD curves and shown in Table 1. It is shown clearly that the cell volume V expands for either martensite or austenite with Nd addition to Ni-Ti binary alloy from 0 at.% to 20 at.%. The observation can also be confirmed in the following composition analysis.

3.2. Morphologies and Compositions of $Ni_{50}Ti_{50-x}Nd_x$ Alloys. Figure 2 depicts the backscattering SEM images of $Ni_{50}Ti_{50-x}Nd_x$ $(x = 0, 1, 3, 7, 20)$ alloys. For Nd0 alloy, there are two different morphologies, namely, black phase and matrix, which can be identified in the SEM image (Figure 2(a)). The black phase is in irregular shape and distributed randomly in the matrix. For Nd1, Nd3, and Nd7, two different morphologies, namely, white phase and matrix, can be identified in the SEM images (Figures 2(b)–2(d)). Some white particles that are nearly round-shape and up to 4 μm, 6 μm and 11 μm in diameter, respectively, with white curving areas can be found to be distributed randomly in the matrix. When the Nd content is 20 at.%, the white phase mainly takes on very irregular shape and becomes larger and interconnected, while some white particles that are nearly round-shaped and up to 14 μm are also found to be distributed in the matrix in Figure 2(e). The size of the white particles evidently increases, whereas the white

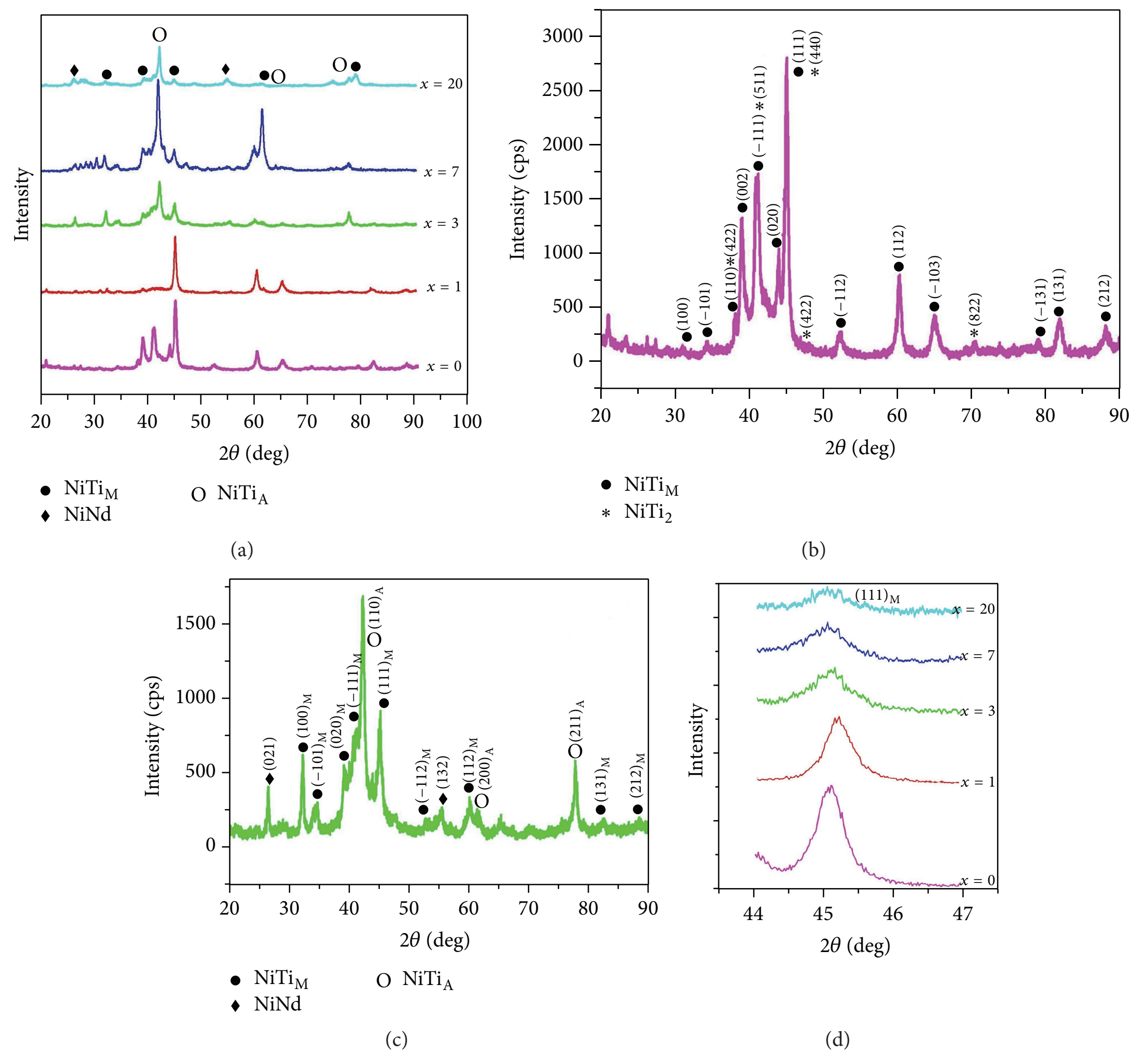

Figure 1: XRD curves of $Ni_{50}Ti_{50-x}Nd_x$ alloys: (a) XRD curves of $Ni_{50}Ti_{50-x}Nd_x$ alloys; (b) indexed diffraction peaks in Nd0; (c) indexed diffraction peaks in Nd3; (d) comparison of $(111)_M$ diffraction peaks of $Ni_{50}Ti_{50-x}Nd_x$ alloys.

phase overspreads steadily on the matrix with increasing Nd fraction.

To identify the boundaries between the white phase and the matrix, TEM observation was conducted for Nd1 alloy and the TEM bright field images of a small nearly round-shaped particle with a diameter of 1.7 μm and a large nearly round-shaped particle with a diameter of 3.6 μm are shown in Figure 3. The boundaries between these two particles and the matrix look very bright and can be identified clearly at such a very low magnification, which means that the boundaries are incoherent. Furthermore, Xu et al. proposed that the binding force of RE elements and Ni is much bigger than that of Ni and Ti [11]. So, NiNd phase is formed first and then NiTi phase crystallization occurs during the Ni-Ti-Nd alloys preparation. Thus NiNd phase and NiTi matrix have no orientation relationship [5].

To identify the phase structure, EDS analysis was conducted in SEM. The compositions of Ni-Ti-Nd alloys are shown in Table 2. The Ti : Ni ratio in the matrix of all Ni-Ti-Nd alloys is measured to be near 1. Thus, the matrix can be concluded to be NiTi phase with a small amount of Nd solute. The Ti : Ni ratio in the black phase of Nd0 alloy is measured to be near 2 : 1. By XRD analysis, there is a $NiTi_2$ phase in Nd0. Thus, the black phase can be concluded to be $NiTi_2$ phase. According to the 773 K isothermal section of the ternary alloy phase diagram of the Ni-Ti-Nd, no intermetallic compounds can be found in the Ti-Nd binary system. However, Ni-Nd binary alloy phase diagram shows seven kinds of intermetallic compounds defined as $NdNi_5$, Nd_2Ni_7, $NdNi_3$, $NdNi_2$, NdNi, Nd_7Ni_{13}, and Nd_3Ni [12]. The EDS results show that the Ni : Nd ratio in the white phase is near 1 and can be regarded as the NiNd intermetallic compound with a small amount of Ti solute. The amount and size of the NiNd phase increase with increasing Nd fraction (Figure 2).

Furthermore, Nd content has also been found in the matrix of Nd3 Nd7, and Nd20. The Nd atomic radius (0.206 nm) is known to be larger than Ti atomic radius

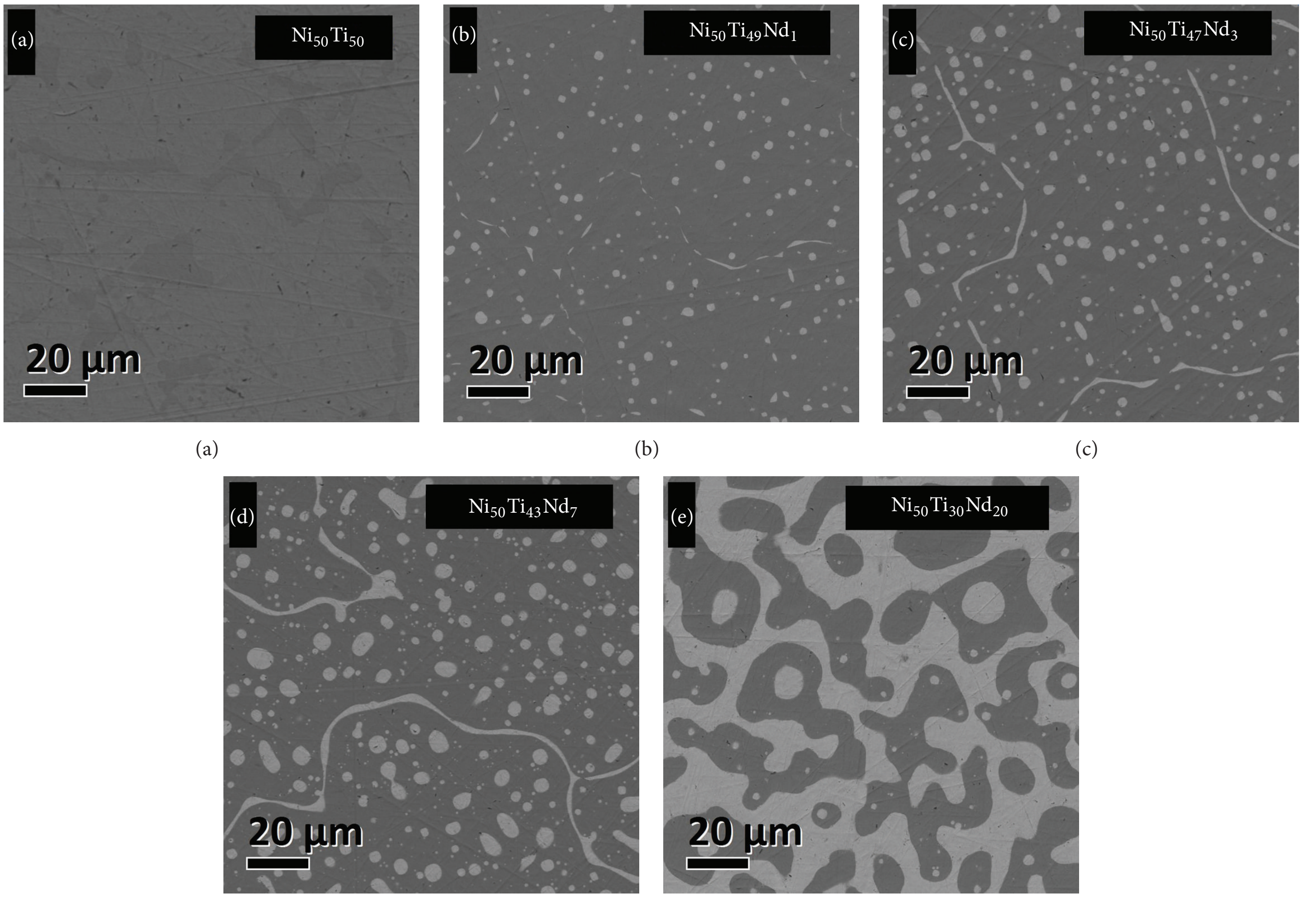

(a) (b) (c)

(d) (e)

Figure 2: Back-scattering SEM images of $Ni_{50}Ti_{50-x}Nd_x$ alloys: (a) $Ni_{50}Ti_{50}$; (b) $Ni_{50}Ti_{49}Nd_1$; (c) $Ni_{50}Ti_{47}Nd_3$; (d) $Ni_{50}Ti_{43}Nd_7$; (e) $Ni_{50}Ti_{30}Nd_{20}$.

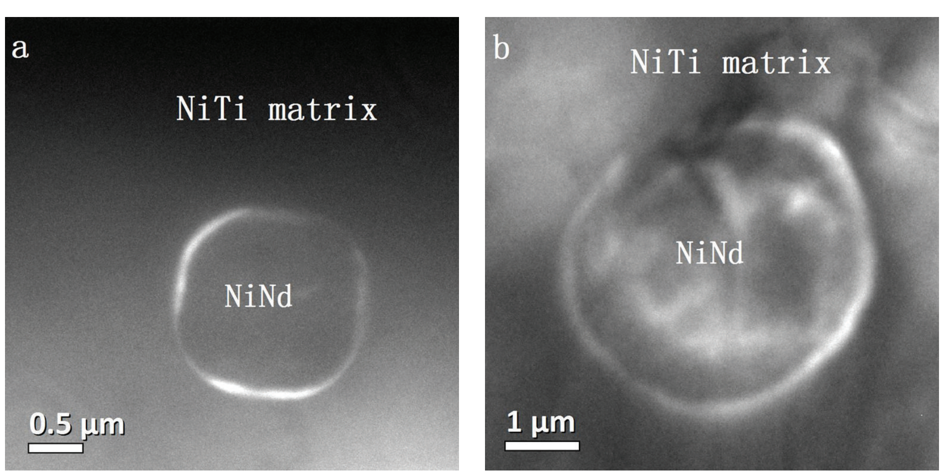

(a) (b)

Figure 3: TEM bright field images of $Ni_{50}Ti_{49}Nd_1$ alloy: (a) small particle; (b) large particle.

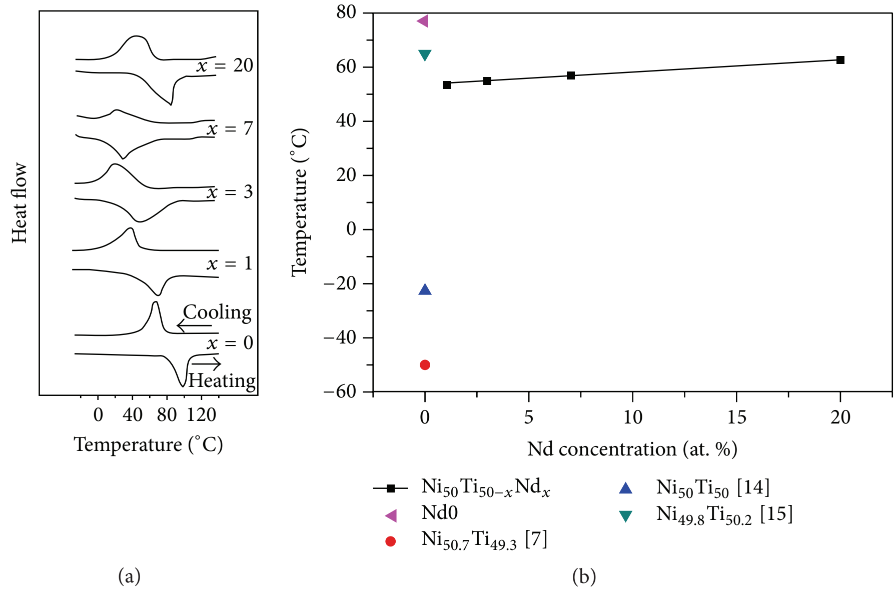

Figure 4: DSC curve and martensite transformation temperature of $Ni_{50}Ti_{50-x}Nd_x$ alloys: (a) DSC curves; (b) M_s curve.

(0.176 nm) by 17% and Ni atomic radius (0.149 nm) by 38% [13]. The Nd atom occupies the position of Ni or Ti, consequentially resulting in an expansion of the NiTi matrix lattice [7], which is consistent with the previous XRD analysis.

3.3. Phase Transformation of $Ni_{50}Ti_{50-x}Nd_x$ Alloys. Figure 4(a) depicts the DSC curves of the $Ni_{50}Ti_{50-x}Nd_x$ ($x = 0, 1, 3, 7, 20$) alloys. Each DSC curve of Nd0, Nd1, Nd3, Nd7, and Nd20 shows only one peak during the heating and cooling process, which indicates a one-step B2↔B19′ phase transformation. Figure 4(b) shows the effect of Nd concentration on martensitic transformation start temperature M_s. For Nd0 alloy, the M_s is measured to be 77.44°C. It is well known that quenched Ni-Ti binary alloys show one-step B2↔B19′ transformation and the transformation temperatures are strongly dependent on Ni concentration [5, 7]. 0.1 at.% increase in Ni concentration can lower the M_s of Ni-Ti binary alloys by more than 10°C. For example, Liu et al. measured the M_s to be about −50°C for $Ni_{50.7}Ti_{49.3}$ alloy after annealing at 900°C for 60 min [7]. Tabish et al. measured the M_s to be −22.12°C for $Ni_{50}Ti_{50}$ alloy after annealing at 1000°C for 120 min [14]. Wasilewski et al. measured the M_s to be 65°C for $Ni_{49.8}Ti_{50.2}$ alloy [15]. In this work, the composition of the matrix in Nd0 is measured to be $Ni_{49.36}Ti_{50.64}$, which is Ti-rich. So, a high M_s of Ti-Ni binary alloy Nd0 is reasonable. Again, the martensite transformations finish temperature M_f in Nd0 alloy is higher than room temperature of 20°C. Thus, the martensite transformations have finished at room temperature and the Nd0 alloy should be in total martensite phase, which is in agreement with the XRD results.

Meanwhile, as shown in Figure 4, the M_s increases with increasing Nd fraction from 1 at.% to 20 at.%. And all M_f in four DSC curves of Nd addition alloys are lower than room temperature. Thus, martensite transformation cannot finish fully at room temperature, which indicates that both the austenite phase and the martensite phase exist in the Ni-Ti-Nd alloy. For Nd1 alloy, the M_f is higher than the others, after which the martensite transformation has nearly finished. Thus, a higher martensite fraction than austenite fraction is present. Consequently, the XRD curve of Nd1 shows that the intensities of the martensite diffraction peaks are significantly higher than those of austenite in Figure 1(a). With increasing Nd fraction, the M_f, the martensite fraction in the alloy, and the relative XRD intensities of the martensite diffraction peaks also decreased.

Table 2: Compositions of Ni-Ti-Nd alloys.

		Ti (at.%)	Ni (at.%)	Nd (at.%)
Nd0	Matrix	50.64	49.36	—
	Black phase	66.99	33.01	—
Nd1	Matrix	50.61	49.39	0
	White phase	5.55	49.67	44.78
Nd3	Matrix	49.24	50.21	0.55
	White phase	2.97	49.84	47.19
Nd7	Matrix	49.99	48.95	1.06
	White phase	4.31	47.72	47.97
Nd20	Matrix	49.27	48.99	1.74
	White phase	1.68	49.78	48.54

4. Conclusions

In summary, the effect of RE element Nd addition on the microstructure and martensitic transformation behavior was investigated by XRD, SEM, TEM, and DSC. The microstructure of the $Ni_{50}Ti_{50-x}Nd_x$ alloys consists of NiNd alloy with a small amount of Ti solute and NiTi matrix with a small amount of Nd solute. The lattice of NiTi matrix is expanded by Nd addition. The Ni-Ti-Nd alloy has a one-step martensitic transformation. Increasing the Nd fraction, the martensitic transformation start temperature M_s increases gradually.

Conflict of Interests

The authors declare that there is no conflict of interests regarding the publication of this paper.

Acknowledgments

This work was supported by the National Natural Science Foundation of China (Grant no. 51261017), the Program for New Century Excellent Talents in University (Grant no. NCET-10-0909), and the Specialized Research Fund for the Doctoral Program of Higher Education (Grant no. 20101514110002).

References

[1] K. Otsuka and X. Ren, "Recent developments in the research of shape memory alloys," *Intermetallics*, vol. 7, no. 5, pp. 511–528, 1999.

[2] J. Frenzel, J. Pfetzing, K. Neuking, and G. Eggeler, "On the influence of thermomechanical treatments on the microstructure and phase transformation behavior of Ni-Ti-Fe shape memory alloys," *Materials Science and Engineering A*, vol. 482–484, no. 1-2, pp. 635–638, 2008.

[3] X. L. Meng, W. Cai, Y. D. Fu, Q. F. Li, J. X. Zhang, and L. C. Zhao, "Shape-memory behaviors in an aged Ni-rich TiNiHf high temperature shape-memory alloy," *Intermetallics*, vol. 16, no. 5, pp. 698–705, 2008.

[4] Y. Liu, M. Kohl, K. Okutsu, and S. Miyazaki, "A TiNiPd thin film microvalve for high temperature applications," *Materials Science and Engineering A*, vol. 378, no. 1-2, pp. 205–209, 2004.

[5] K. Otsuka and X. Ren, "Physical metallurgy of Ti-Ni-based shape memory alloys," *Progress in Materials Science*, vol. 50, no. 5, pp. 511–678, 2005.

[6] W. Cai, A. L. Liu, J. H. Sui, and L. C. Zhao, "Effects of cerium addition on martensitic transformation and microstructure of $Ti_{49.3}Ni_{50.7}$ alloy," *Materials Transactions*, vol. 47, no. 3, pp. 716–719, 2006.

[7] A. L. Liu, W. Cai, Z. Y. Gao, and L. C. Zhao, "The microstructure and martensitic transformation of $(Ti_{49.3}Ni_{50.7})_{1-x}Gd_x$ shape memory alloys," *Materials Science and Engineering A*, vol. 438–440, pp. 634–638, 2006.

[8] A. L. Liu, Z. Y. Gao, L. Gao, W. Cai, and Y. Wu, "Effect of Dy addition on the microstructure and martensitic transformation of a Ni-rich TiNi shape memory alloy," *Journal of Alloys and Compounds*, vol. 437, no. 1-2, pp. 339–343, 2007.

[9] J. W. Xu, A. L. Liu, B. Y. Qian, and W. Cai, "Investigation on microstructure and phase transformation of La added TiNi shape memory alloy," *Advanced Materials Research*, vol. 557–559, pp. 1041–1044, 2012.

[10] J. G. Wang and F. S. Liu, "Phase transformation and microstructure of $Ti_{50}Ni_{48-x}Fe_2Nd_x$ shape memory alloys," *Chinese Journal of Aeronautics*, vol. 22, no. 3, pp. 334–338, 2009.

[11] J.-W. Xu, A.-L. Liu, and W. Cai, "Crystal structure and formation mechanism of rare earth rich phases in Ti-Ni-Ce alloys," *Journal of Functional Materials*, vol. 39, no. 4, pp. 600–602, 2008 (Chinese).

[12] J. Q. Liu, Y. H. Zhuang, and Y. Q. Hu, "The 773 K isothermal section of the ternary phase diagram of the Nd-Ni-Ti," *Journal of Alloys and Compounds*, vol. 368, no. 1-2, pp. 180–181, 2004.

[13] E. Clementi, D. L. Raimondi, and W. P. Reinhardt, "Atomic screening constants from SCF functions. II. Atoms with 37 to 86 electrons," *The Journal of Chemical Physics*, vol. 47, no. 4, pp. 1300–1307, 1967.

[14] T. A. Tabish, S. Atiq, M. Ali, A. N. Ch, Z. U. Reham, and T. Z. Butt, "Development and characterization of $Ni_{50}Ti_{50}$ shape memory alloy used for biomedical applications," *International Journal of Chemical, Materials Science and Engineering*, vol. 7, no. 12, pp. 92–93, 2013.

[15] R. J. Wasilewski, S. R. Butler, and J. E. Hanlon, "On the martensitic transformation in TiNi," *Metallurgical Transactions*, vol. 1, no. 1, pp. 104–110, 1967.